Double precision errors in the logistic map: Statistical study and dynamical interpretation

J. A. Oteo*
Departament de Física Teórica, Universitat de València, 46100-Burjassot, València, Spain

J. Ros†
Departament de Física Teórica and Instituto de Física Corpuscular, Universitat de València, 46100-Burjassot, València, Spain

(Received 25 June 2007; published 26 September 2007)

The nature of the round-off errors that occur in the usual double precision computation of the logistic map is studied in detail. Different iterative regimes from the whole panoply of behaviors exhibited in the bifurcation diagram are examined, histograms of errors in trajectories given, and for the case of fully developed chaos an explicit formula is found. It is shown that the statistics of the largest double precision error as a function of the map parameter is characterized by jumps whose location is determined by certain boundary crossings in the bifurcation diagram. Both jumps and locations seem to present geometric convergence characterized by the two first Feigenbaum constants. Eventually, a comparison with Benford's law for the distribution of the leading digit of compilation of numbers is discussed.

DOI: 10.1103/PhysRevE.76.036214 PACS number(s): 05.45.Pq, 05.10.−a, 05.45.−a

I. INTRODUCTION

Among the different approaches used to study dynamical systems, numerical simulations play a distinguished role. Important as they are, however, numerical experiments often appear tinged with a shade of doubt. This applies even to simple discrete systems where the evolution is calculable by direct iteration without recourse to further algorithms. The reason, obviously, is the inherent limitations due to the computer finite precision [1,2]. Rigorous studies such as shadowing theorems [3], in some way, tend to restore confidence in the numerical approach. However, their applicability is not general and extension by numerical analysis has only been partially successful [4,5].

A great majority of numerical studies in nonlinear science are still done in the IEEE 64-bit floating-point arithmetic standard, which provides 53 mantissa bits, or approximately 16-decimal-digit accuracy and is commonly referred to as *double precision* (DP). It is interesting then to assess the effects of these inaccuracies in the study of the dynamics of a system. In this paper we present a careful statistical analysis of the errors made when the trajectories in the logistic map are computed in DP.

To appraise the validity of DP calculations one has to be able to compare these results with either explicit exact solutions, which is rarely possible, or high-precision floating-point calculations. To this end use can be made of high-precision software packages. Commercial symbolic programming languages such as MAPLE or MATHEMATICA may certainly be useful. We have instead used the specialized high-precision arithmetic package MPFUN [6] which allows to arbitrarily increase the precision at a lower computational cost. Notice that using high-precision software rises markedly computer run times. For MPFUN, beyond 100-digit precision, the computational cost for p digits precision goes as p^2 up to 1000 digits [7]. In the present work, we have carried out 400-digits-accuracy computations in the critical loops of the codes, referred to as MP for short.

Strictly speaking the finite precision of computer simulations results in a finite discretization of phase space and correspondingly in the impossibility of truly chaotic trajectories. This consideration has been the starting point of many investigations following the work by Rannou [8] and different aspects concerning the logistic map can be found in [9–13]. These references study the partition in cycles of the finite phase space and its behavior with the number of states. It differs from our main goal which, as already stated, focus on the dependence of the errors made in DP calculations on the control parameter. To the best of our knowledge, this is a topic hardly touched upon in the literature.

The numerical problems mentioned above are perfectly illustrated with the familiar logistic map: after only 50–60 iterations calculated in DP the trajectory may differ sensibly from the exact one. This known fact is illustrated in Sec. II, where the general setting of our calculations is presented.

In Sec. III, we pinpoint some particular values of the logistic map parameter corresponding to the onset of chaos, period 3, period 6, intermittency and fully developed chaos, which allow us to illustrate that in spite of the errors in the trajectories the invariant density is a stable magnitude beyond DP. It constitutes an instance of shadowability in the logistic map.

In Sec. IV the statistics of numerical errors made in DP computations is presented. Section V contains an analysis of the statistics of the largest numerical error that occurs in DP computations. A connection with the bifurcation diagram is established and a geometric convergence phenomenon described. A comparison of some of our results with Benford's law for the statistics of the most significant digit of compilation of numbers is given in Sec. VI. Eventually, Sec. VII contains our conclusions.

II. NUMERICS

The logistic map is defined by the iteration

*oteo@uv.es
†rosj@uv.es

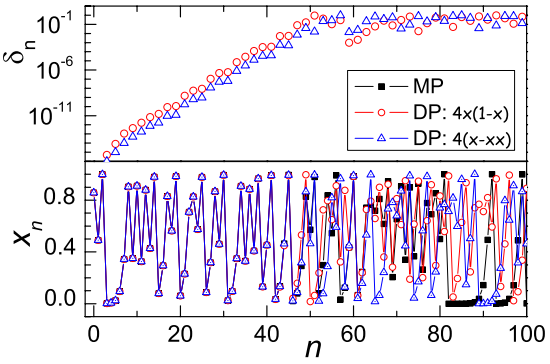

FIG. 1. (Color online) Trajectory x_n of the logistic map with parameter $r=4$ (lower panel). Initial value $x_0=0.857$. Square symbols stand for the analytic solution Eq. (2) or, equivalently, the MP numerical computation of the logistic map. Circles (red) represent DP computation of Eq. (1). Triangles (blue) represent DP computation of Eq. (3). With the same symbols code, the upper panel shows in semilogarithmic scales the absolute error of both DP computations for the 100 first iterations.

$$x_{n+1} = rx_n(1 - x_n) \equiv f(x_n, r), \tag{1}$$

with $r \in [0,4]$ and $x_n \in [0,1]$. The system with $r=4$ has the explicit solution for the nth iteration,

$$x_n = \sin^2(2^n \arcsin \sqrt{x_0}), \tag{2}$$

in terms of the initial value x_0. As a matter of fact, there exist explicit solutions [14,15] for any value of r. They are given by expressions much more involved that Eq. (2) and so are not of any practical use for our discussion.

In the bottom panel of Fig. 1 we have plotted an instance of the first 100 iterations for the logistic map with $r=4$. The open circles stand for the DP computation of Eq. (1). The solid squares stand for the MP computation starting from the same initial condition. It is clear that after 50 iterations both computations differ markedly. The open circles in the upper panel show, in logarithm scale, the absolute difference of the value between both computations at every iteration.

Equation (2) should serve as a control test of both computations. In practice, however, the round-off errors in its evaluation render it useless as such a test in DP. Since MPFUN allows an evaluation of Eq. (2) for $n>50$ we are able to assess the number of iterations for which MP computations remain *exact*. In general, the number of iterations preserving p digits goes as $3.3p$. We presume that for values $r<4$ the behavior is similar and choose to use runs up to 1200 iterations in order to guarantee the *exactness* of the numeric MP series. Nevertheless we buttress the procedure by performing a further numerical test. The loss of computer precision may be interpreted, at a more abstract level, as the breaking of the associative and distributive properties of real number algebra [16]. To detect this breaking we have programmed concurrently a *distributed* version of the logistic map in Eq. (1), namely

$$x_{n+1} = r(x_n - x_n x_n), \tag{3}$$

which is handled by the compiler differently from Eq. (1). Differences in the trajectories between Eq. (1) and Eq. (3) conveys a numeric precision failure. The open triangles in Fig. 1 stand for the DP computation of Eq. (3). We observe that the trajectories given by Eq. (1) and Eq. (3) move away after 50–60 iterations. Instead, no warning of this kind was found in any of the runs up to 1200 iterations when MP was used. It is then safe to take MP results as exact. The open triangles in the upper panel of Fig. 1 stand for the absolute error in the trajectory from Eq. (3).

At first sight, the scenario depicted above seems certainly not very promising. Fortunate enough, results based on shadowing theorems [3] establish that the set of numerical orbits can be shadowed by true orbits for long time periods. More specifically, in [3] it is shown with the help of the computer that if the logistic map (and, in general, low dimensional maps) is iterated with $2p$-digits accuracy there is a true orbit $\{y_n\}$ within a distance 10^{-p} of $\{x_n\}$ for an average of 10^p iterates (i.e., $n=0,1,2,\ldots,10^p$) before separation. According to this, statistical magnitudes such as the histograms associated to the invariant densities should, *a fortiori*, be preserved. We perform explicit verifications of it in the next section, which paves the road to study the main subject of the paper, namely, the statistics of the numerical errors of trajectories computed in DP for different values of r.

III. INVARIANT DENSITIES AND TRAJECTORIES

The well-known bifurcation diagram for the logistic map presents a rich variety of behaviors as the control parameter varies [17]. Next we analyze what happens for particular values of r. The purpose is to illustrate that the invariant density is preserved in DP. This is in contrast with the fact that numerical trajectories may move away from true ones after a number of iterations. This description will help us in the discussion of the statistics of errors that is carried out in the next sections.

A. Fully developed chaos

At $r=4$ any point $x \in [0,1]$, except a set of zero measure, belongs to the chaotic attractor. In this case the invariant density has explicit solution [18]. It reads

$$\rho(x) = \frac{1}{\pi\sqrt{x(1-x)}}. \tag{4}$$

The scattered points in Fig. 2 stand for histograms of the invariant density. Open circles and solid squares correspond to DP and MP computations, respectively. They were obtained from one thousand runs of 1200 iterations each, from equally spaced initial conditions. To avoid transient effects, the first 600 points of every run were ruled out. The solid line stands for the function $300\pi\rho(x)$. A similar figure, just for DP, is found in [18]. The invariant density seems to be preserved in spite of the divergences in trajectories.

B. The edge of period 3

At the value $r=1+\sqrt{8}$ a transition from chaos to a stable period-3 regime takes place *via* intermittency [19]. This phenomenon is characterized by a tangent bifurcation and its

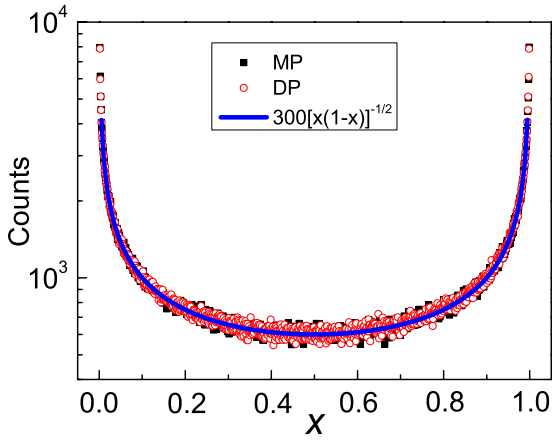

FIG. 2. (Color online) Histograms for the invariant density of the logistic map (1) with parameter $r=4$. Black solid (red open) symbols stand for MP (DP) computations. The blue solid line is the function $300\pi\rho(x)$. A DP computation with Eq. (3) yields a similar histogram.

effect on trajectories can be observed in Fig. 3 where irregular bursts are intermingled with period-3-like segments, for the value $r=1+\sqrt{8}-10^{-3}$. Notice that except for the first iterations (lower panel) the sequences of bursts are different in DP and MP, even thought the numerical value for the initial point is the same. However, the invariant density, for which histograms are plotted in the lower panel of Fig. 4, seems to coincide. Notice from the upper panel of Fig. 4 the strict correspondence between the location of the periodic orbit and the main histogram cusps below. This is an instance of subduction [19].

C. The edge of period 6

A transition from chaos to a period-6 regime occurs, via intermittency, around the value $r=3.6265$. The situation is similar to that of period 3. In Fig. 5 we represent DP and MP histograms of the invariant density just before (bottom panel)

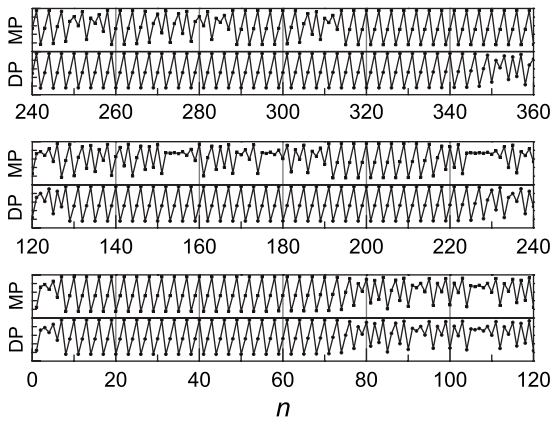

FIG. 3. Snapshots of a chaotic trajectory up to $n=360$ at the edge of the period-3 window: $r=1+\sqrt{8}-10^{-3}$ exhibiting intermittency. Bottom (top) subpanels correspond to DP (MP) computations. The initial point is the same for both computations, $x_0=0.25$. Vertical scales (nonlabeled) stand for the interval [0,1].

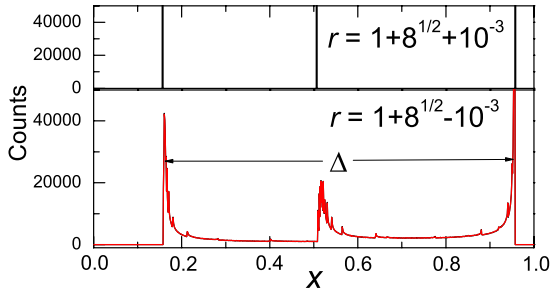

FIG. 4. (Color online) DP and MP histograms of invariant densities at the edge of period 3. Top panel is for $r=1+\sqrt{8}+10^{-3}$, regular stable regime. Bottom panel is for $r=1+\sqrt{8}-10^{-3}$, chaotic regime: only the color online version allows a tiny difference between DP (red line) and MP (black line) to be observed. Arrows bound the largest error Δ found, defined in Sec. IV, which holds for both panels.

and after (top panel) the tangent bifurcation. Again, notice the consonance between the position of the periodic orbit and cusps of the histograms below. The DP and MP histograms seem to coincide here too.

We have considered this case for it is an instance of invariant density that spawns two well separated segments of $x\in[0,1]$, where $\rho(x)\neq 0$, which we will refer to as *clusters*. This fact will be useful to illustrate the nature of DP numerical errors.

D. The edge of chaos

A cascade of pitchfork bifurcations, which duplicate the period of trajectories, occurs at values $r=3,3.449\,490,3.544\,090,3.564\,407,\ldots$. As is well known, these locations converge geometrically to the value $r_\infty=3.569\,945\,672\ldots$, which is usually referred to as the *edge of chaos*. The ratio of the intervals between successive bifurcation tends asymptotically to the first Feigenbaum constant [20]. The invariant density $\rho(x)$, or rather histograms standing for it in numerical computations, are composed of simply isolated discrete peaks. Beyond r_∞ structures that connect some combinations of those peaks emerge, and eventually *macroscopic* clusters appear. Their size continue to increase

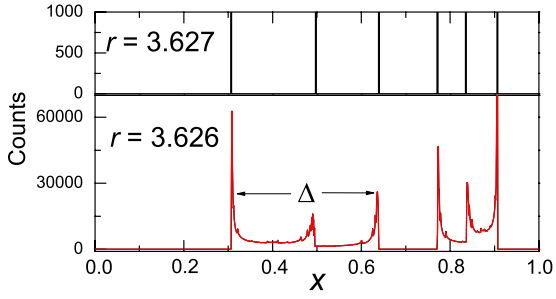

FIG. 5. (Color online) DP and MP histograms of invariant densities at the edge of period 6. Top panel is for $r=3.627$, regular regime. Bottom panel is for $r=3.626$, chaotic regime: only the color online version allows one to notice a tiny difference between DP (red line) and MP (black line). Arrows delimit the largest error Δ, defined in Sec. IV. This value holds also for the upper panel.

with r and occasionally two clusters merge. The last merging, in that sequence, occurs at $r_* \sim 3.678$, and may also be clearly detected on the bifurcation diagram in Fig. 8 [see panel 8(b)]. The merging of clusters just mentioned will be further discussed in Sec. V.

E. Near bifurcation points

When examined at a sufficient magnification level, the lines near pitchfork bifurcation points of the logistic map in the bifurcation diagram exhibit *anomalous* broadening. Such closeups reveal smooth lines instead of the abrupt bifurcation theoretically expected. We deem pertinent to point out that this is an effect due to the transient regime and not to the finite precision computation.

A plausible explanation to this phenomenon stems from the fact that near a pitchfork bifurcation to period 2^n

$$\left| \frac{d}{dx} f^{[n]}(x,r) \right| \approx 1, \tag{5}$$

and thus the rate at which a point reaches the periodic attractor is low. Here $f^{[n]}$ stands for the nth iteration of f.

IV. STATISTICS OF DP ERRORS

Let us define the absolute error in a DP computation of the logistic map at the iteration n as

$$\delta_n(r) \equiv |x_n^{MP} - x_n^{DP}|, \tag{6}$$

where the superscript refers to the numerical precision achieved in the computation of the sequence $\{x_n\}$. For r fixed we generate 5000 runs of 1200 iterations starting from equally spaced initial values on the unit interval.

The preservation of $\rho(x)$ in DP computations allows us to establish generic bounds to the magnitude of δ_n errors.

We commence by distinguishing DP errors in regular stable regimes from chaotic ones. In periodic orbits, an output $\delta_n > 0$ may only come from an entry in a wrong location of the attractor. Thus, the DP orbit is globally correct but there is a lag between it and the MP orbit. In the worst of cases, δ_n equals the distance between the two outermost points of the orbit.

By the same token, errors in chaotic regimes will be bounded by the distance between outermost borders of the attractor. We will show, however, that there exists a wide domain of r values where numerical errors are not so wild as they could at first be.

Next we present the results for the statistics of DP errors in a number of chaotic regimes.

A. Case $r=4$

The probability distribution of errors $\delta_n(r)$ in the case $r=4$, fully developed chaos, admits analytical solution on the basis of the invariant density in Eq. (4).

To obtain an explicit formula we will suppose that δ_n is a random variable. Let x_n be the DP value and y_n the exact value. Since both of them are distributed according to Eq. (4), the probability P of obtaining a value z for the error reads

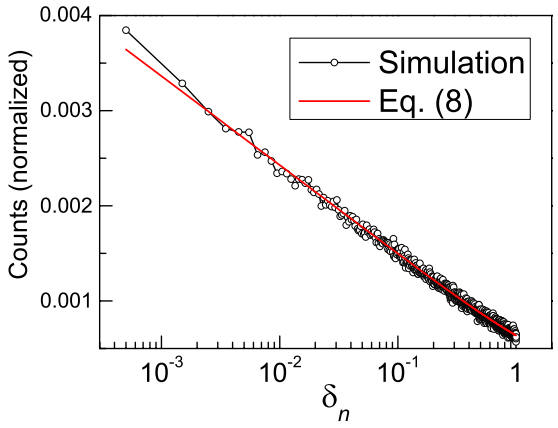

FIG. 6. (Color online) Error statistics of DP trajectories of the logistic map, Eq. (1), with parameter $r=4$ are represented by circles. The solid straight line (blue) stands for the analytic formula, Eq. (8). Computations from Eq. (3) yield similar results and are not given for the sake of clarity.

$$P(z) = \int_0^1 \int_0^1 \rho(x)\rho(y)\delta(|x-y|-z)dxdy. \tag{7}$$

After some computations, Eq. (7) yields

$$P(z) = \frac{8}{\pi^2(1+z)} K\left[\left(\frac{z-1}{z+1}\right)^2\right], \tag{8}$$

where K stands for the complete elliptic integral of the first kind [21]. In Fig. 6 we have plotted $P(z)$ for the same abscissaes than the numerical simulation, normalized to sum one. That is the solid, approximately straight, line. The circles in Fig. 6 correspond to the histogram of errors $\delta_n(4)$, normalized to one. The agreement with Eq. (8) is remarkable. We observe that, although the logistic map in DP is error prone, large errors are less likely than small ones. Notice the striking linear dependence on $\log_{10}(\delta)$ over three magnitude orders.

B. Cases $r \neq 4$

The case $r=4$ is exceptional in that $\rho(x)$ assumes a smooth shape, unlike the cases $r \neq 4$ where it is difficult to imagine common functions describing a lot of cusps. The results of numerical simulations are plotted in Fig. 7. We have computed the errors for $r=3.6, 3.7, 3.8, 3.9$. The case $r=4$ has been included for the sake of comparison. As already stated above, we observe that the largest error decreases with r as a consequence of the shrinking of the attractor. This is the subject of the next section.

V. STATISTICS OF THE LARGEST ERROR

The statistics of the largest error as a function of r presents some interesting features. For fixed value of r we define the largest error $\Delta(r)$ as the largest one obtained among

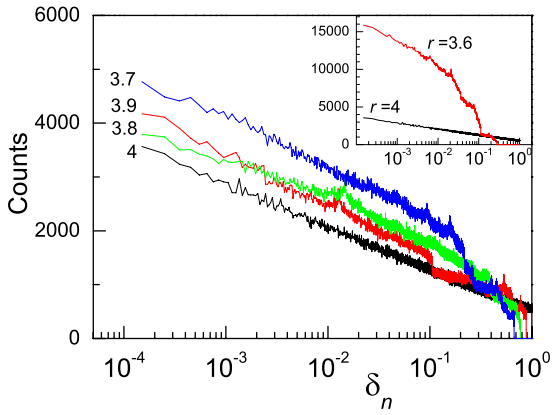

FIG. 7. (Color online) Histograms of the error [see Eq. (6)] statistics of DP trajectories of the logistic map. Results for several parameter values are shown. Curves are explicitly labeled with the value of r for the sake of clarity. The inset shows the case $r=3.6$ which is off scale.

the 5000 runs of 1200 iterations each. The result is given in panel Fig. 8(a). The abscissas are in terms of $R \equiv r - r_\infty$, namely the value of r referred to the point r_∞, the onset of chaos. The inset stands for the same curve in log-log scales. The sudden jumps in Δ coincide with the merging of two clusters in $\rho(x)$. This may be put in visual correspondence with the bifurcation diagram in Fig. 8(b), at least for the rightmost discontinuities. Comparing a number of $\rho(x)$ histograms for various values of r with the corresponding $\Delta(r)$ we have observed that whenever various (disjoint) clusters

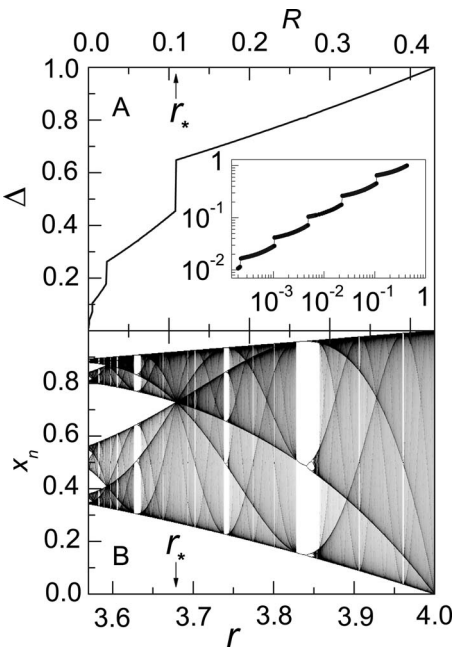

FIG. 8. (a) Largest error Δ in the DP precision computation of the logistic map as a function of $R \equiv r - r_\infty$. The inset corresponds to the same curve in log-log scales. (b) Bifurcation diagram for the logistic map. Abscissas start at $r=r_\infty$, which establishes the proper axes correspondence with (a) and allows one to observe that the discontinuities in $\Delta(r)$ correlate with the merging of segments of $\rho(x)$.

exist, which means $r < r_*$, then $\Delta(r)$ is simply given by the size of the widest one. This is in contrast with what we would have expected, namely $\Delta(r)$ to be determined by the distance between the two outermost points of the attractor, a behavior that does indeed occur for $r > r_*$. Notice that trajectories do not need to stay trapped in any cluster.

Furthermore, it is interesting that for values of $r > r_\infty$ corresponding to periodic stable windows of the logistic map there is no sudden decreasing of Δ, even though it is a regular regime. This is the consequence of a long transient before entering the periodic attractor. For some initial conditions, the transient exceeds the quoted number of 50 *bona fide* iterations supported by DP. After that, it is likely that the trajectory enters the periodic attractor at the wrong point. What seems even more striking is that the system keeps memory of the chaotic regime immediately before subduction. We have explicitly pointed out this feature in Figs. 4 and 5.

A worth mentioning issue about the inset of Fig. 8(a) concerns the approximate power law followed by the largest DP errors as a function of R. Furthermore, this plot inset has a twofold striking feature. Namely, the logarithm of both (i) the horizontal length spawned by the curved segments, and (ii) the size of the jumps at discontinuities, are approximately constant. This fact certainly reminds the geometric convergence characteristic of the period doubling route to chaos at the *other side* of r_∞. Indeed, when the period doubling cascade of the bifurcation diagram of the logistic map is plotted with respect $\log_{10}|r - r_\infty|$, the distances between bifurcation points become approximately constant [18], and a similar effect occurs on the vertical scale. All this, as is well known, yields the two first universal Feigenbaum constants: $\delta_F = 4.669\ldots$ (bifurcation velocity parameter) and $\alpha_F = 2.503\ldots$ (reduction parameter) [22].

In view of the evidence, we have investigated the existence of bifurcation velocity and reduction parameters in the data in Fig. 8(a). Notice that here *bifurcations* cascade in the opposite direction, towards decreasing values of r. To this end we have determined directly from our data the (approximate) values of the discontinuities D_n in $\Delta(r)$ and the points R_n where they take place. Here $n=1$ refers to the last merging, located at r_*, and $n=2,3,\ldots$ refer to previous merging $\{r_*^{(n)}\}$ to the left of $r_* \equiv r_*^{(1)}$. The parameters δ_{DP} and α_{DP}, in case of existing, are defined here by the equations

$$R_n = C_R \delta_{DP}^{-n}, \tag{9}$$

$$D_n = C_D \alpha_{DP}^{-n}, \tag{10}$$

for some constants C_R, C_D. In Fig. 9 we have plotted the four pairs of data for the Δ discontinuities we have obtained. Linear fits to $\log_{10}(R_n)$ and $\log_{10}(D_n)$ give the estimations $\delta_{DP} = 4.69 \pm 0.02$ and $\alpha_{DP} = 2.48 \pm 0.02$, indeed very close to δ_F and α_F, respectively. Of course, so far this is only based on numerical exploration and no rigorous renormalization group analysis has been developed. A similar behavior has been observed for other observables [10]. The results which follow from our identification of Δ with the size of the largest cluster size in $\rho(x)$ could have been expected as a manifes-

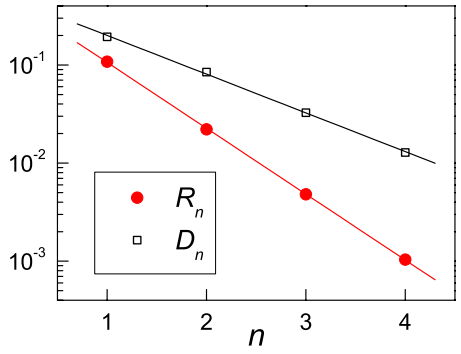

FIG. 9. (Color online) Semilogarithmic plot for relative location R_n of jumps in $\Delta(r)$ and height of discontinuities D_n. Linear fits are suggested by Eqs. (9) and (10).

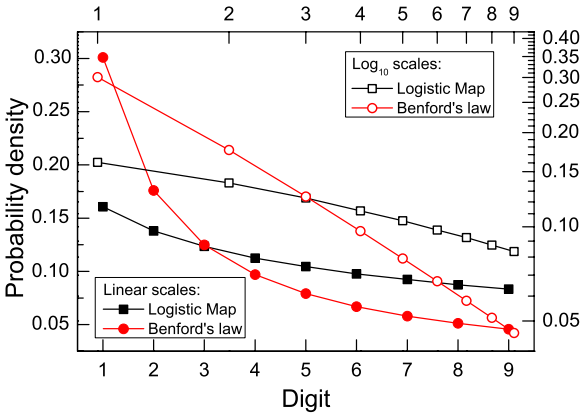

FIG. 10. (Color online) Leading digit statistics from the logistic map errors (squares) and Benford's law (circles). Solid symbols are referred to linear scales (bottom and left axes). Empty symbols are referred to $\log_{10}$-$\log_{10}$ scales (top and right axes).

tation of the *band splitting phenomenon* described in detail in [23].

We have, at several places in this paper, mentioned the connection between the isolated clusters in the invariant density on one hand, and the statistical results for DP errors on the other hand. At this point we can reinforce this connection with more quantitative considerations. This will strengthen our conclusions.

The darker lines clearly visible in Fig. 8(b) correspond to peaks of $\rho(x)$. They are known as *boundaries* [24,25] and are given by the curves $f^{[n]}(1/2,r)$, the locus generated after n iterations of the logistic map starting at its critical point $x=1/2$. For $n=1,2$ they form the exterior boundaries of the bifurcation diagram for $r>r_\infty$ and are the lines $r/4$ (uppermost boundary) and $r(4-r)/16$ (lowermost boundary). For $n\geqslant 3$ they are termed *internal* and their crossings correspond to fixed or periodic points (stable or unstable) eventually attracting the critical point. So, for example, $f^{[3]}(1/2,r)=f^{[4]}(1/2,r)$ signals out a fixed point ($x=1-1/r$) and this occurs, in the range of r values of our interest, at $r_*\equiv r_*^{(1)}=3.678\,573\,510\ldots$, which is the value obtained from the data mentioned in Sec. III D. In an analogous way $f^{[5]}(1/2,r)=f^{[7]}(1/2,r)$ furnishes $r_*^{(2)}=3.592\,572\,184\ldots$, and the critical point ends up in an unstable cycle of period two. We have also determined the next interesting crossing of boundaries, $f^{[9]}(1/2,r)=f^{[13]}(1/2,r)$, occurring for $r_*^{(3)}=3.574\,804\,938\ldots$, sending the critical point to a period four cycle. All these values $\{r_*^{(n)}\}$, $n=1,2,3$, do agree with our data in Fig. 8. The analytic form of the different segments of $\Delta(r)$ can be obtained in terms of polynomials. However their degree increase quickly as r decreases. For $r_*<r<4$ one trivially gets obtains $\Delta(r)=r(2-r)^2/16$. For $r_*^{(2)}<r<r_*$ one can easily check that $\Delta(r)=f^{[4]}(1/2,r)-r^2(4-r)/16$, which is a polynomial of degree 15. In both cases the agreement with the simulation data in Fig. 8 is perfect. This numerical agreements give sound basis to our interpretation of the results of the numerical simulation.

VI. BENFORD'S LAW

Benford's law [26,27] is a heuristic result which states that the probability P_B for d, with $d=1,2,\ldots 9$, to be the most significant digit (the leftmost, nonzero digit in a number) in compilation of numbers reads

$$P_B(d)=\log_{10}(1+1/d) \tag{11}$$

Thus, the digit 1 appears about one third of the time whereas the digit 9 appears less than one time in twenty. Due to the logarithmic dependence this law exhibits scale invariance and for this reason the unit system chosen or the radix do not matter [27]. The law does not apply for a list of numbers drawn, for instance, from normal distributions. Instead, Benford's law works better when the numbers originate from distributions selected at random and random samples are taken from them.

It is clear from Fig. 6 that the set of DP errors $\{\delta_n(4)\}$ has scale invariance when we consider the intervals $\{[0.1,1],[0.01,0.1],[0.001,0.01]\}$: inside every interval, errors with a specific leading digit occur with the same relative frequency, independently of the interval in question. However, that invariance differs from Benford's law. To verify this issue, we have build up a Benford-like histogram with the DP numerical errors from 5000 runs of 1200 iterations long which started from equally spaced initial conditions. The first 600 iterations of every run were considered as a transient sequence. Eventually, the histogram was normalized to unity so as to make a fair comparison with Benford's law, Eq. (11). The results are plotted in Fig. 10 with dual scales. Solid symbols are referred to left and bottom linear scales. A clear difference is observed between both curves. If DP numerical errors were a pure random variable, every digit should appear with the same probability, which corresponds to a horizontal line at height equal to 1/9.

Figure 10 shows the results also in log-log scales (top and right axes). Both curves exhibit approximate power laws. The value of the slope of Benford's law is about three times greater than that of the logistic map.

The most widely accepted explanation for Benford's law states that it emerges whenever a wide variety of distinct distributions enters in the generation of the set of numbers. What the results in Fig. 10 tell us is that the set of involved

distributions in the DP computation, whatever it may be, seems not enough to fit Benford's law. DP errors in the logistic map are halfway between pure random and Benford's.

VII. CONCLUSIONS

We have analyzed the statistics of the unavoidable numerical errors in the DP computations of the logistic map. We have illustrated that the invariant density is preserved, in spite of the fact that 50 iterations may be more than enough to ruin a DP computation from the point of view of precision in trajectories. This result is buttressed by shadowing theorems.

The statistics of DP errors δ_n shows that they follow approximately a linear distribution with $\log_{10}(\delta_n)$. Although the DP computation is error prone, large errors are much less likely than small ones.

The analysis of the largest numerical DP error points out that the relevant range $r \in [0,4]$ can be partitioned in three subsets. For $0 \leqslant r < r_\infty$ there are no significant errors. For $r_\infty \leqslant r < r_*$, the largest error is given by the size of the longest connected subset in the support of the invariant density. It results in a monotonically increasing function of r with jumps corresponding to the merging of clusters. Finally, for $r_* \leqslant r \leqslant 4$, Δ is given by the maximum separation between points in the attractor, which increases continuously with r.

It is noteworthy that the DP accuracy of regular trajectories is different depending on whether r is either to the left or to the right of r_∞. Whereas before the edge of chaos numerical errors in the trajectory remain small, at the level of the DP accuracy, once the edge of chaos is surpassed that accuracy level is no longer ensured. Definitely, for $r > r_*$ some initial conditions whose transient lasts more than (say) 50 iterations do enter the periodic attractor at the wrong place. One could say to this respect that across a tangent bifurcation the system keeps memory of the chaotic character of the preceding regimen, as regards DP numerics. The well-known phenomenon of intermittency that occurs in these transitions may be observed in MP as well as in DP computations.

Incidentally, we have established a relationship between these jumps of $\Delta(r)$ in the interval $r_\infty \leqslant r < r_*$ and the location of particular boundary crossings in the bifurcation diagram (merging points) and is connected to the *band splitting phenomenon*. The determination of bifurcation velocity and reduction parameters we have carried out gives numerical values very close to the first two Feigenbaum constants. The existence of these constants witnesses a geometric convergence phenomenon.

In the case of fully developed chaos we have established that the DP errors in the logistic map do not follow Benford's law. Interestingly, the probability density in Eq. (8), based on the complete elliptic integral of the first kind K, could be viewed as a type of distribution preserving scale invariance that is halfway between Benford's and pure random behavior. This would be most likely the case when not enough distribution laws intervene in the generation of the numbers under scrutiny.

In summary, we have shed some light on the effects that the unavoidable numerical accuracy limitations may have in some critical loops of programming codes. Concomitantly, we have shown that multiprecision software may efficiently help to control this respect within reasonable amounts of CPU time. To close this work we would like to highlight the utility that this kind of tool could have in the computations of complex systems, where to the best of our knowledge it has not found use.

ACKNOWLEDGMENTS

This work has been partially supported by Contracts MCyT/FEDER, Spain (Grant No. FIS2004-0912) and Generalitat Valenciana, Spain (Grant No. ACOMP07/03). We thank R. Guardiola for a careful reading of the manuscript.

[1] R. C. Hilborn, *Chaos and Nonlinear Dynamics* (Oxford University Press, Oxford, 2000).
[2] E. R. Scheinerman, *Invitation to Dynamical Systems* (Prentice-Hall, Englewood Cliffs NJ, 1996).
[3] S. M. Hammel, J. A. Yorke, and C. Grebogi, J. Complex. **3**, 136 (1987).
[4] E. M. Coven, I. Kan, and J. A. Yorke, Trans. Am. Math. Soc. **308**, 227 (1988).
[5] C. Grebogi, S. M. Hammel, J. A. Yorke, and T. Sauer, Phys. Rev. Lett. **65**, 1527 (1990).
[6] D. H. Bailey, ACM Trans. Math. Softw. **19**, 288 (1993).
[7] D. H. Bailey, Comput. Sci. Eng. **7**, 54 (2005).
[8] F. Rannou, Astron. Astrophys. **31**, 289 (1974).
[9] P. M. Binder and R. V. Jensen, Phys. Rev. A **34**, 4460 (1986); P. M. Binder, Physica D **57**, 31 (1992).
[10] C. Beck and G. Roepstorff, Physica D **25**, 173 (1987).
[11] P. Diamond, P. Kloeden, A. Pokrovskii, and A. Vladimirov, Physica D **86**, 559 (1995).
[12] G. Yuan G., and J. A. Yorke, Physica D **136**, 18 (2000).
[13] M. Falcioni, A. Vulpiani, G. Mantica, and S. Pigolotti, Phys. Rev. Lett. **91**, 044101 (2003).
[14] S. Rabinovich *et al.*, Physica A **218**, 457 (1995).
[15] M. Bruschi, J. Phys. A **31**, L153 (1998).
[16] J. F. Colonna, Commun. ACM **36**, 15 (1993).
[17] See, for example, S. H. Strogratz, *Nonlinear Dynamics and Chaos* (Perseus Books, Cambridge, MA, 1994).
[18] P. Collet and J. P. Eckmann, *Iterated Maps on the Interval as Dynamical Systems* (Birkhäuser, Boston, 1980).
[19] C. Grebogi, E. Ott, and J. A. Yorke, Physica D **7**, 181 (1983).
[20] M. Feigenbaum, J. Stat. Phys. **19**, 25 (1978); **21**, 669 (1979).
[21] *Handbook of Mathematical Functions With Formulas, Graphs, and Mathematical Tables*, edited by M. Abramowitz and I. A. Stegun (Dover, New York 1972).
[22] *The On-Line Encyclopedia of Integer Sequences*, http://www.research.att.com/~njas/sequences/, see sequences A006890 and A006891.

[23] C. Beck and F. Schlögl, *Thermodinamics of Chaotic Systems* (Cambridge University Press, Cambridge, 1993).
[24] R. V. Jensen and C. R. Myers, Phys. Rev. A **32**, 1222 (1985).
[25] J. Eidson, S. Flynn, C. Holm, D. Weeks, and R. F. Fox, Phys. Rev. A **33**, 2809 (1986).
[26] F. Benford, Proc. Am. Philos. Soc. **78**, 551 (1938).
[27] T. Hill, Proc. Am. Math. Soc. **123**, 887 (1995).